Journal of Chromatography, 301 (1984) 107–128
Elsevier Science Publishers B.V., Amsterdam — Printed in The Netherlands

CHROM. 16,919

COMPUTERISED GAS CHROMATOGRAPHIC–MASS SPECTROMETRIC ANALYSIS OF COMPLEX MIXTURES OF ALKYL PORPHYRINS

P. J. MARRIOTT*, J. P. GILL, R. P. EVERSHED, C. S. HEIN and G. EGLINTON*
Organic Geochemistry Unit, University of Bristol, School of Chemistry, Cantock's Close, Bristol BS8 1TS (U.K.)
(Received May 15th, 1984)

SUMMARY

Computerised capillary gas chromatography–mass spectrometry (GC–MS) analysis of complex mixtures of alkyl porphyrins, as their bis-(trimethylsiloxy)silicon(IV) and bis(*tert.*-butyldimethylsiloxy)silicon(IV) derivatives, is described. The latter derivative is more suitable for routine GC–MS analysis.

This computerised GC–MS approach, when applied to the alkyl porphyrins of two geological samples, a bitumen (Gilsonite, Eocene age, UT, U.S.A.) and a crude oil (Boscan, Cretaceous age, West Venezuela), has revealed the highly complex compositions of these fractions. Computer-aided data processing, using relative retention index (RRI) calculations, facilitated the classification of the chromatographic peaks according to structural type and membership of pseudo-homologous series.

Computerised GC–MS is compared with, and contrasted to high-performance liquid chromatography as a means of petroporphyrin analysis.

INTRODUCTION

Alkyl porphyrins occur widely in crude oils and sedimentary materials as complexes of nickel (as Ni^{2+}), vanadium (as $V=O^{2+}$) and, to a lesser extent, other metal ions (*e.g.* copper, gallium, iron and manganese)[1–3]. Free-base porphyrins have also been observed in certain deep-sea sediments[4]. These porphyrins, referred to as petroporphyrins, usually occur as complex mixtures. Electron impact probe mass spectrometry (EI probe MS) with accurate mass measurement has revealed what appear to be homologous, or more likely pseudo-homologous series (a pseudo-homologous series is a group of related compounds in which the formulae of preceding and succeeding members differ by one methylene group, but where the methylene group difference is not confined to a common alkyl chain) of at least five structurally related types of alkyl porphyrin[5,6]. The two main series are structurally related to the aetio (1) and DPEP (2) porphyrins originally proposed by Treibs[8,9] on the basis of ultra

* Present address: Department of Chemistry, National University of Singapore, Kent Ridge, Singapore.

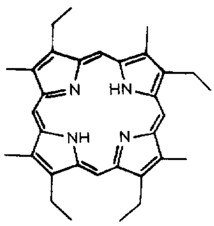
1

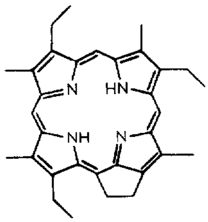
2

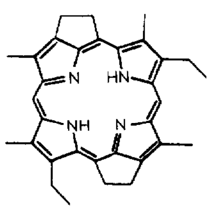
3

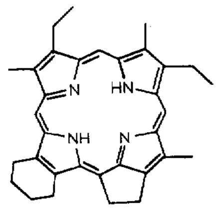
4

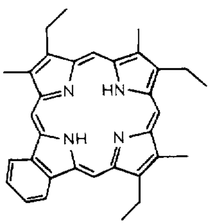
5

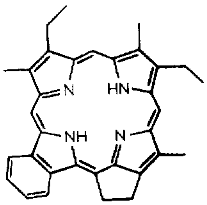
6

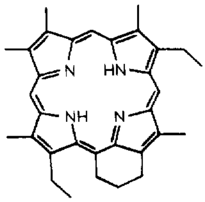
7

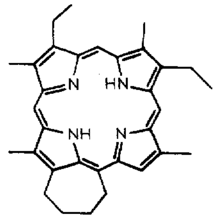
8

violet/visible (UV–vis) spectrophotometry and elemental analyses. Three minor series have also been observed and classified as di-DPEP (3 or 4), rhodo-aetio (5) and rhodo-DPEP (6) type porphyrins[5–7]. Although the EI probe MS technique reveals structural type and carbon number (C_n) ranges, it is unable to distinguish between structural isomers of a given molecular formula. However, thin layer chromatography (TLC) and high performance liquid chromatographic (HPLC) fractionation followed by MS (including hydrogen chemical ionisation MS (H_2-CI-MS) and nuclear magnetic resonance spectroscopic (NMR) determinations have recently established the presence of structural isomers of various molecular formulae in sedimentary materials[10–13].

An efficient chromatographic technique is required to resolve these complex mixtures in order that both qualitative and quantitative assessment of the petroporphyrin compositions can be made for the purposes of geochemical analysis. Although the polarity-based normal phase HPLC of free-base porphyrins is capable of resolving individual C_n homologues and structural isomers, the identification of the eluting components requires lengthy trapping and subsequent EI probe MS[10]. Linked liquid chromatography–MS (LC–MS) would offer a solution to these problems, but while the LC–MS of petroporphyrins has been demonstrated it is not yet perfected nor widely available[14]. Recent improvements in interface design have increased the potential of this technique[15].

In the late 1960's Boylan and Calvin[16] and Boylan *et al.*[17] showed that alkyl porphyrins could be gas chromatographed on packed columns as bis(trimethylsiloxy)-Si(IV) derivatives. Recognising the potential of this technique, in the light of improved column technology and the wide availability of computerised gas chromatography–mass spectrometry (GC–MS), it was decided to pursue this technique as a means of petroporphyrin analysis. During the course of this development work we have successfully gas chromatographed synthetic porphyrin standards both as free-bases[18] and as a wide variety of metal complexes[19–21]. Of the derivatives that have been tested, the bis(trialkylsiloxy)Si(IV) complexes originally developed by Boylan and Calvin[16] showed greatest suitability for petroporphyrin analysis[21]. They elute at relatively low retention index (between tricontane (n-C_{30}) and tetracontane (n-C_{40}) on apolar stationary phases, compared to greater than pentacontane (n-C_{50}) for free-bases and other metal complexes) with GC peak shapes comparable in quality to those of n-alkanes of similar retention index[18–21].

Derivatives of this type have now been successfully applied to the analysis of the petroporphyrins of Gilsonite bitumen and Boscan crude oil[22]. Described herein are the sample preparation and computerised GC–MS procedures for the analysis of these complex alkyl porphyrin mixtures. The relative suitabilities of the trimethylsilyl (TMS) and *tert.*-butyldimethylsilyl (TBDMS) derivatives for petroporphyrin analysis are discussed, as are the techniques for the interpretation of the MS and retention data.

EXPERIMENTAL

Extraction and purification of petroporphyrins

The porphyrins of crude oils and bitumens were extracted as their free-bases by demetallation with methanesulphonic acid (MSA), according to the procedure of Erdman[23].

Typically, crude oil (1 g) was heated (100°C, 4 h) with at least a five-fold excess of MSA (98%, Aldrich, 5–10 ml). The reaction was quenched by pouring the acid–oil mixture into distilled water (20 ml). After allowing to cool, the coagulated organic material was removed by filtration. This organic residue was washed with aliquots of dilute MSA (3 × 5 ml; 50% v/v), until the filtrate was colourless. The combined aqueous extracts, containing the porphyrins as dications, were extracted with dichloromethane (DCM, 3 × 5 ml), neutralised ($NaHCO_3$) and dried (Na_2SO_4). The free-bases obtained in this way were purified by TLC (silica gel) or Sep-Pak (Waters Assoc.; silica gel), using dichloromethane as eluant.

Dihydroxysilicon(IV) porphyrin formation

The insertion of silicon into an aliquot of the free-base porphyrins obtained above, was carried out by a modification of the method of Marriott *et al.*[21]. The free-base porphyrins (1 mg) were dissolved in dry toluene (1 ml) in a screw-topped vial and hexachlorodisilane (Si_2Cl_6; 1 drop, Aldrich) added. Quantitative formation of the dichlorosilicon(IV) porphyrins occurred in 2 h at room temperature as indicated by the presence of visible absorption maxima at 535 and 574 nm (DCM) and absence of absorbance bands corresponding to free-base or porphyrin dications.

Hydrolysis of the dichlorosilicon(IV) porphyrins to their corresponding dihydroxy complexes was achieved by pouring the reaction mixture into saturated aqueous potassium hydroxide (5 ml). Once effervescence had ceased and all solids dissolved, the toluene was decanted from the aqueous layer. The aqueous layer was then extracted with DCM (3 × 5 ml). The toluene and DCM extracts containing the dihydroxysilicon(IV) porphyrins were combined and evaporated to dryness. Purification by TLC (Alumina H; dichloromethane; R_F = 0.3) was performed prior to silylation of the axial hydroxyl groups.

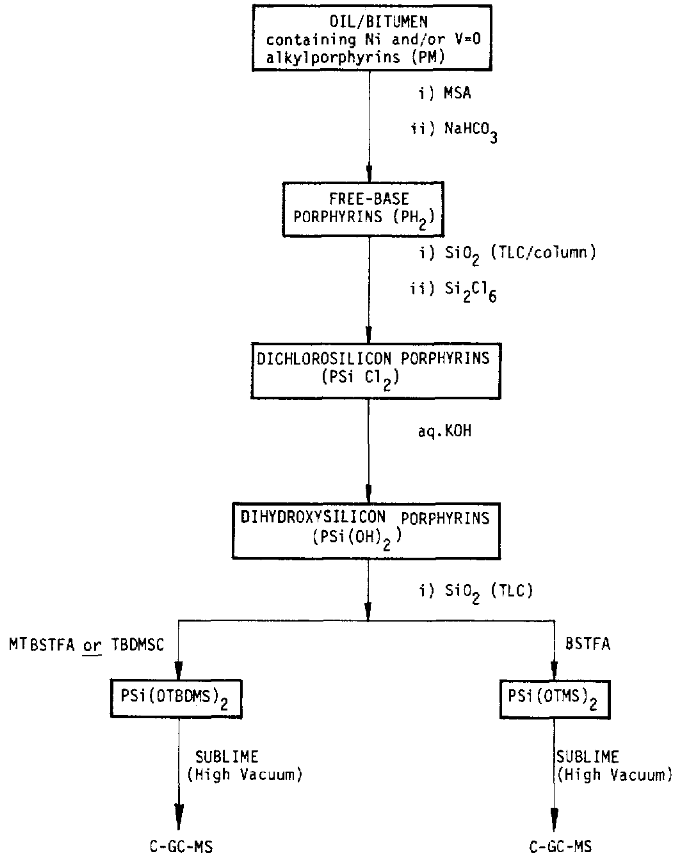

Fig. 1. Scheme for the extraction, demetallation and derivatisation of petroporphyrins for computerised GC–MS. TBDMSC = *tert.*-Butyldimethylchlorosilane; MTBSTFA = N-methyl-N-(*tert.*-butyldimethylsilyl)trifluoroacetamide; BSTFA = N,O-bis(trimethylsilyl)-trifluoroacetamide; MSA = methanesulphonic acid.

Silylation

Silylations were performed by the methods described previously[21]. Recently, however, N-methyl-N-(*tert.*-butyldimethylsilyl)trifluoroacetamide (MTBSTFA: Regis Chemical Co.) has been used in place of Corey's reagent[24] to form the bis(*tert.*-butyldimethylsiloxy)silicon(IV) porphyrins (abbreviated to $(TBDMSO)_2Si(IV)$). In this modified silylation procedure the MTBSTFA (2 drops) was added to a solution of the dihydroxysilicon(IV) porphyrin (0.1 mg) in dry pyridine (0.3 ml) and heated (60°C; 10 h). After evaporation of the pyridine the derivatised porphyrins were dissolved in hexane and decanted. Evaporation of the hexane followed by sublimation (*ca.* 10^{-6} Torr, 125°C, 1 h) removed volatile impurities. Sublimation of the porphyrins (*ca.* 10^{-6} Torr, 175°C) separated them from involatile impurities. (These extraction and derivatisation procedures are summarised schematically in Fig. 1.)

Instrumentation

Two computerised GC–MS systems were employed in this work:

(1) A Carlo-Erba FTV 4160 gas chromatograph, fitted with Grob-type split/splitless and on-column injectors, was interfaced to an AEI MS30 double focusing magnetic sector mass spectrometer through a modified flexible silica interface system, the details of which are described elsewhere[21].

(2) A Finnigan 9610 gas chromatograph equipped with a modified SGE OCI-2 on-column injector linked to a Finnigan 4000 mass spectrometer.

Each of these GC–MS systems was under the control of a Finnigan INCOS 2300 data system.

GC columns

A number of capillary columns were employed in this work; these ranged from 6–25 m in length and were mainly fused silica (0.3–0.34 mm I.D.) coated with OV-1 (0.17 μm film-thickness). The columns were supplied by both Hewlett Packard and Phase Separations. Good results were also obtained on a Chrompack CPSil 5 coated glass capillary (20 m × 0.32 mm I.D.). Helium was the carrier at gas velocities of 50–100 cm sec^{-1}. All analyses were temperature programmed.

Retention index calculation

Co-chromatography with *n*-alkanes (C_8–C_{44}; Phase Separations) permitted subsequent computer calculation of relative retention indices (RRI) for the eluting alkyl porphyrin derivatives. Relative retention indices were calculated in a manner similar to the Kovat's method and will be referred to as pseudo-Kovat's retention indices (KRI). The operation of the retention index algorithm is to first determine the two retention index standards between which a given component elutes, then to determine more precisely the KRI value of that component via the formula:

$$\mathrm{RI}(X) = \left[\frac{\mathrm{RT}(X) - \mathrm{RT(PI)}}{\mathrm{RT(SI)} - \mathrm{RT(PI)}} \times (\mathrm{RI(SI)} - \mathrm{RI(PI)})\right] + \mathrm{RI(PI)} \qquad (1)$$

Where: RT = retention time = scan number in MS file; RI = retention index; X = given point in RT; PI = RI standard preceding X; SI = RI standard succeeding X, which simplifies for KRI calculation to[25]:

$$\mathrm{KRI(PP)} = \left[\frac{\mathrm{RT(PP)} - \mathrm{RT}(\mathrm{C}_n)}{\mathrm{RT}(\mathrm{C}_{n+1}) - \mathrm{RT}(\mathrm{C}_n)} \times 100\right] + 100n \qquad (2)$$

Where: C_n and C_{n+1} are the *n*-alkanes of carbon number n and $n + 1$, which preceed and succeed petroporphyrin (PP) derivative of interest.

This relative retention index calculation algorithm is used in various FORTRAN programs to produce:

(1) Listings of peak areas, retention indices and reduced mass spectra (referred to as the relative retention index listing (RRIL) program).

(2) Plots of ion current profiles along a KRI scale (referred to as the relative retention index multiple plotting (RRIM) program in which retention time (= scan number in GC–MS file) is converted to KRI).

(3) Graphs of porphyrin C_n *vs.* KRI for the various structural types.

(4) Histogram profiles along a KRI scale for single C_n isomer distributions or pseudo-homologous series (analogous to 2).

The use of the KRI conversion techniques simplifies comparison of various samples by providing a basis for matching components from one computerised GC–MS run to those of another. More detailed description of these computer programs will be given in a future publication.

RESULTS AND DISCUSSION

Selection of TBDMS vs. TMS derivatives for porphyrin GC–MS

Assessments of the relative suitabilities of the TMS and TBDMS derivatives for computerised GC–MS analysis have been performed, employing synthetic alkyl porphyrins [aetioporphyrin-I and octaethylporphyrin (OEP)]. On balance, the TBDMS is considered to be the derivative of choice for petroporphyrin analysis. The properties of the two derivatives are compared below in terms of their ease of formation, solvolytic and thermal stability, GC retention behaviour and mass spectral characteristics.

Derivative formation. TMS ethers are universally acknowledged to form in near quantitative yield using reasonably mild conditions (*i.e.* taking up the solute in the TMS reagent (such as BSTFA) with or without additional solvent). The more sterically hindered TBDMS species may not necessarily be produced quantitatively[26], though there is no evidence of low yield when the porphyrins are derivatised with TBDMS reagents.

Stability. The TBDMS derivatives are believed to be in the order of 10^4 times more stable to solvolysis than the TMS derivatives of hydroxy functionalities[27]. For the silicon porphyrins there seems to be evidence to suggest that hydrolysis of the TMS is facile, thus requiring repeated BSTFA treatment.

The observed temperature stabilities of these two derivatives also point to the superiority of the TBDMS. Although there is no evidence of compound loss in the column at the temperature of analysis, the TMS would appear to suffer from thermal degradation in hot split/splitless injectors, at least above about 200°C. The alternative TBDMS derivative is more resistant to the rigours of flash volatilisation, so making it more compatible with narrow bore capillary columns for which on-column injectors are unsuited.

Retention volumes. The TMS derivatives of silicon porphyrins elute *ca.* 380 retention units earlier than the TBDMS analogues, therefore TBDMS derivatives require programming to higher temperatures in the GC and GC–MS analyses if they are to elute in similar times after the onset of isothermal conditions in the programme (of the order of 15°C more for TBDMS). This difference in temperature requirements is trivial; the normal temperature used is 300°C and this does not appear to damage columns coated with appropriate high temperature apolar phases.

Mass spectrometry requirements (in GC–MS analysis). TBDMS derivatisation adds 262 atomic mass units (a.m.u.) to the basic porphyrin–silicon structure, whilst TMS adds only 178 mass units. For example, for a C_{36} aetio porphyrin, its $(TBDMSO)_2Si(IV)$ derivative has MW = 822, with the $(TMSO)_2Si(IV)$ derivative only 738. The significant ions for the TMS derivatives are the molecular ion (M) and the M − 89 ion (*i.e.* for loss of one axial ligand; Fig. 2A). For $(TMSO)_2SiOEP$ these

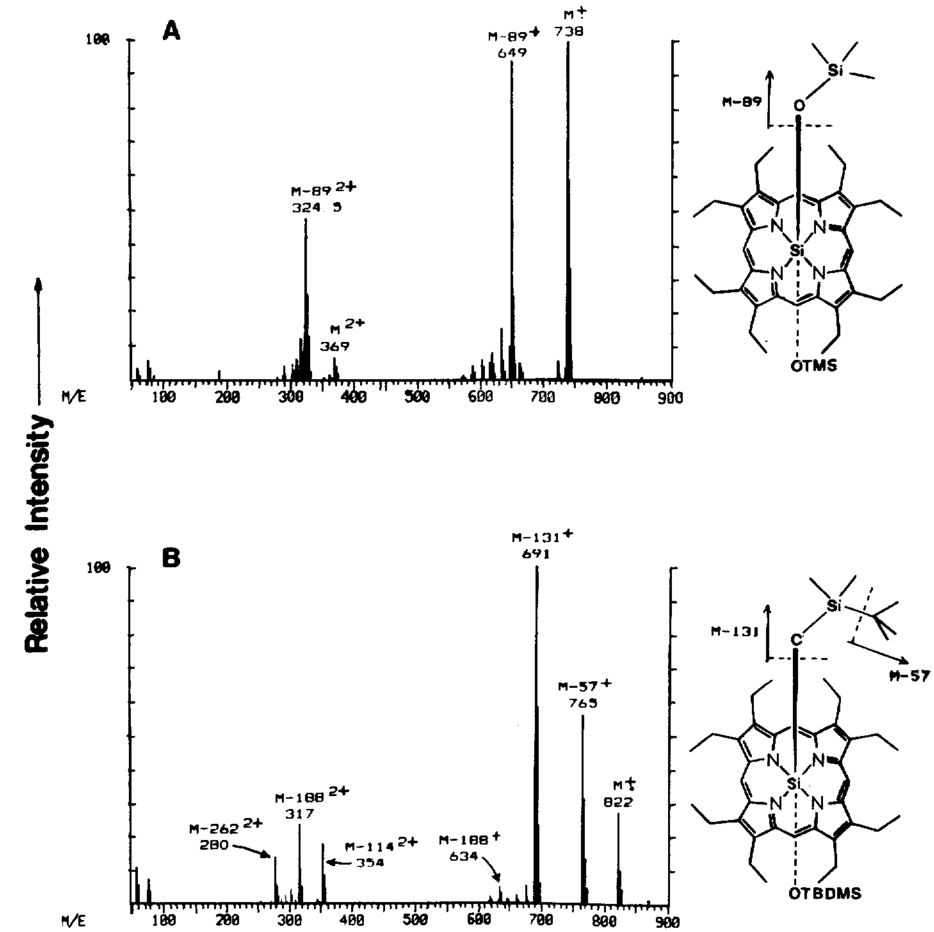

Fig. 2. Mass spectra for (A) the $(TMSO)_2Si$ and (B) the $(TBDMSO)_2Si$ derivatives of octaethylporphyrin, obtained by direct insertion probe MS on the MS 30 spectrometer. The ionisation and accelerator voltages were maintained at 40 eV and 3.2 kV, respectively, while employing a source temperature of 200°C, source pressure 10^{-7} Torr and a total scan time of 4.5 sec.

are 738 and 649, respectively. From the molecular ion, the loss of 15 mass units may be observed, whereas from the M − 89 ion additional losses of multiples of 15 mass units (for benzylic cleavage of the ethyl substituents) are found. For $(TBDMSO)_2SiOEP$ (Fig. 2B), the observed ions are at 822 ($M^{+\cdot}$), 765 $(M - 57)^+$ and 691 $(M - 131)^+$, with the latter two for cleavage of the *tert.*-butyl group (−57) and loss of the axial ligand (−131). In spectra recorded on magnetic instruments (*e.g.* MS 30) the base peak is invariably the ion (M − 131) corresponding to loss of one axial ligand, and the molecular ion is of the order of 30% or less of the base peak (Fig. 2B). In the case of the quadrupole instrument (*e.g.* Finnigan 4000) the molecular and M − 57 ions were of lower intensity (generally ⩽ 7 and 25% respectively) than for the magnetic instrument. The M − 131 ion contains as much information as the molecular ion regarding the identity of the porphyrin type (aetio or DPEP, etc.) and the number of carbons on the macrocycle (though not the substituent arrangement around the tetrapyrrole). Since the M − 131 fragment carries so much of the ion intensity in the mass spectrum, then it should be a useful ion to use for analytical purposes for the TBDMS derivative. This compares with the observation of two rather large ions in the mass spectrum of TMS derivatives, where for trace components both ions may be lost rather than having one stronger ion as in TBDMS. Hence it is only necessary to scan up to the maximum value expected for the $(M - 131)^+$ species (*i.e.* about 700 m/z) in the case of the TBDMS derivatives. A further loss of 57 a.m.u. occurs from the M − 131 ion (*i.e.* loss of *tert.*-butyl group from the other axial ligand (M − 188)) and the benzylic cleavages leading to loss of methyl groups commonly seen for free base porphyrins are not so prevalent for the M − 131 ion of these derivatives. The relative absence of these complicating fragmentations is an attractive point when dealing with complex natural samples.

In summary, the TBDMS derivative is preferred for the analysis of complex porphyrin mixtures owing to its excellent GC and MS characteristics. The higher thermal stability makes this derivative more amenable to split/splitless injection at high temperature, thereby allowing the use of narrow bore columns offering higher efficiency and, hence, improved component resolution.

Petroporphyrin analysis

Both the TMS and TBDMS derivatives have been successfully applied to the

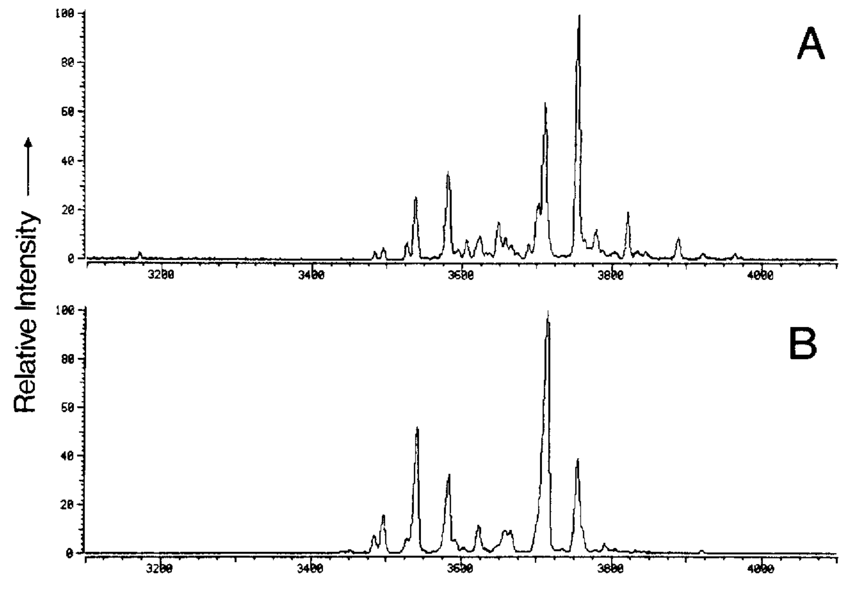

Fig. 3. Total porphyrin GC–MS traces for Boscan crude oil (A) and Gilsonite bitumen (B), obtained by computer summation of ions in the mass range 550–850. The analyses were performed on a new 25 m × 0.3 mm I.D. OV-1 coated (0.17 μm) flexible silica capillary (Hewlett-Packard), using helium as carrier gas at a linear flow-rate of 50 cm sec^{-1}. Following on-column injection of 2–5 μg of porphyrins as their $(TBDMSO)_2Si(IV)$ derivatives, the GC oven temperature was programmed ballistically from ambient to 150°C, then from 150–290°C at 3°C min^{-1}. The retention time scale has been converted to KRI by computer interpolation from coinjection *n*-alkanes.

analysis of mixtures of petroporphyrins[18,22]. For the reasons outlined above, the TBDMS derivative has been adopted for routine analysis. The mass chromatograms resulting from the computerised GC–MS analysis of the TBDMS derivatives of the porphyrins of the Gilsonite bitumen and Boscan crude oil are shown in Fig. 3. These chromatograms display only the peaks corresponding to the petroporphyrin derivatives. Such chromatograms result from the computer summation of the ions in the m/z range 550–850. This range encompasses the major fragment ions $(M - 131)^+$ and $(M - 57)^+$ of the porphyrin derivatives in the C_n range C_{26}–C_{42} (see Table I). The m/z 550–850 chromatogram is regarded as the total "porphyrin" mass chromatogram. In Fig. 3 the mass chromatograms are plotted along a KRI scale; this is of considerable help when comparing independent analyses.

Normal-phase (SiO_2) HPLC analyses have revealed at least 30 individual petroporphyrin components for Gilsonite and more than 60 for Boscan[10]. The mass chromatograms displayed in Fig. 3 for these two samples show considerably fewer individual peaks, as a result of GC co-elution. Detailed examination of the "porphyrin" chromatograms by mass fragmentography (MF) and through the mass spectra of the individual peaks confirms this observation. The apparent poor peak shapes seen for each of the samples undoubtedly arise through the large number of co-eluting or only partially resolved components. The excellent GC peak shapes afforded by the individual porphyrin components can be seen in the mass fragmentograms (Fig. 4).

Data interpretation

The power of computerised GC–MS as a technique for petroporphyrin analysis lies in its ability to resolve the many co-eluting components through computerised MF. The mass fragmentograms (Fig. 4) plotted for the petroporphyrin derivatives of Boscan petroleum are for the individual intense $(M - 131)^+$ ions (Table I). Many of these plots show a multiplicity of peaks corresponding to elution of isomers of a given carbon number. Where these peaks are genuinely structural isomers of the same molecular formula, then the mass fragmentograms can be regarded as a relative abundance distribution of these isomers plotted against increasing retention time. However, ions having the "characteristic" masses chosen to generate the mass fragmentograms can arise in other ways (see Table II). Therefore to check that a given mass fragmentogram peak represents only $(M - 131)^+$ ions, the following screening procedure has been adopted. This procedure is shown schematically in Fig. 5.

Firstly, mass fragmentograms are plotted for single m/z values corresponding to the $(M - 131)^+$ base peaks (Table I). The full MS data scans for each distinguishable peak in the total porphyrin chromatogram (*i.e.* Fig. 3A or 3B), usually 10–15 scans, are summed. This gives a spectrum which can then be interpreted on the basis of the known fragmentations of porphyrin standards (*e.g.* Fig. 2B) with reference to the listing (Table I) of calculated masses for fragment ions. By way of example the summed mass spectrum for the shaded peak (KRI 3755–3800) of the Boscan run is shown in Fig. 6. The spectrum reveals that this peak comprises seven co-eluting components: five DPEP-type porphyrins in the C_{29}–C_{33} range, and two aetio porphyrins (C_{33} and C_{34}). The characteristic $(M - 131)^+$ ion can be seen for all seven of these components and forms the basis of the assignment. The presence of five of the components is confirmed by the detection of lower intensity fragment

TABLE I

CALCULATED MASSES FOR THE $(M-131)^+$, $(M-57)^+$ AND $M^{+\cdot}$ IONS OF ALKYLPORPHYRINS AS THEIR BIS-(*tert.*-BUTYLDIMETHYLSILOXY)Si (IV) DERIVATIVES

*Carbon number** *(C_n)*	*Porphyrin type (m/z)*					
	Aetio			*DPEP*		
	$(M-131)^+$	*$(M-57)^+$*	*$M^{+\cdot}$*	*$(M-131)^+$*	*$(M-57)^+$*	*$M^{+\cdot}$*
20	467	541	598	465	539	596
21	481	555	612	479	553	610
22	495	569	626	493	567	624
23	509	583	640	507	581	638
24	523	597	654	521	595	652
25	537	611	668	535	609	666
26	551	625	682	549	623	680
27	565	639	696	563	637	694
28	579	653	710	577	651	708
29	593	667	724	591	665	722
30	607	681	738	605	679	736
31	621	695	752	619	693	750
32	635	709	766	633	707	764
33	649	723	780	647	721	778
34	663	737	794	661	735	792
35	677	751	808	675	749	806
36	691	765	822	689	763	820
37	705	779	836	703	777	834
38	719	793	850	717	791	848
39	733	807	864	731	805	862
40	747	821	878	745	819	876
41	761	835	892	759	833	890
42	775	849	906	773	847	904

* Total number of carbon atoms in porphyrin nucleus and β-alkyl substituents.

ions $(M - 57)^+$ and three of these by their $M^{+\cdot}$ ions. Weak $(M - 188)^+$ ions (*i.e.* the loss of *tert.*-butyl (*m/z* 57) from the $(M - 131)^+$ ion) are detected only for the more abundant C_{31} and C_{32} DPEP components. Peaks corresponding to these seven co-eluting components are clearly visible in the region of their $(M - 131)^+$ mass fragmentograms (Fig. 4) for which the mass spectrum was recorded. It is also notable that peaks for the C_{31}–C_{33} aetio and, C_{27} and C_{28} DPEP derivatives are visible in this region of the fragmentograms (Fig. 4). Fig. 6 shows that these peaks in the fragmentograms are not due to $(M - 131)^+$ fragment ions but correspond to ^{13}C-containing fragment ions. Examples of isobaric (co-incident mass) fragment ions are given in Table II. Each of the peaks in the mass fragmentograms shown in Fig. 4 have been screened in the above manner. Those corresponding to "genuine" $(M - 131)^+$ peaks are shaded. In addition to the aetio and DPEP components shown in Fig. 4, a number of derivatives of porphyrins of masses corresponding to the proposed di-DPEP, rhodo-aetio and rhodo-DPEP types have also been observed in Boscan. Only aetio, DPEP and di-DPEP components have been detected in Gilsonite. These porphyrin analyses yield a substantial volume of mass spectral and retention data, further analysis of which is aided by computer processing.

Di-DPEP			*Rhodo-aetio*			*Rhodo-DPEP*		
$(M-131)^+$	$(M-57)^+$	$M^{+\cdot}$	$(M-131)^+$	$(M-57)^+$	$M^{+\cdot}$	$(M-131)^+$	$(M-57)^+$	$M^{+\cdot}$
463	537	594	461	535	592	459	533	590
477	551	608	475	549	606	473	547	604
491	565	622	489	563	620	478	561	618
505	579	636	503	577	634	501	575	632
519	593	650	517	591	648	515	589	646
533	607	664	531	605	662	529	603	660
547	621	678	545	619	676	543	617	674
561	635	692	559	633	690	557	631	688
575	649	706	573	647	704	571	645	702
589	663	720	587	661	718	585	659	716
603	677	734	601	675	732	599	673	730
617	691	748	615	689	746	613	687	744
631	705	762	629	703	760	627	701	758
645	719	776	643	717	774	641	715	772
659	733	790	657	731	788	655	729	786
673	747	804	671	745	802	669	743	800
687	761	818	685	759	816	683	757	814
701	775	832	699	773	830	697	771	828
715	789	846	713	797	844	711	785	842
729	803	860	727	801	858	725	799	856
743	817	874	741	815	872	739	813	870
757	831	888	755	829	886	753	827	884
771	845	902	769	843	900	767	841	898

Computerised data processing

The co-chromatography with *n*-alkane mixtures in the porphyrin analyses permitted computerised interpolation in KRI calculations for the porphyrins appearing as peaks in the $(M - 131)^+$ mass fragmentograms and subsequently validated by detailed examination of the full mass spectra. FORTRAN programs have been developed which present this KRI data either graphically as ion current (IC) plots along a KRI scale (Fig. 3, RRIM display) or as a numerical listing of peak areas, reduced MS, scan numbers and KRI (Fig. 7; RRIL output). Both these forms of the data are of considerable value in the processing of the computerised GC–MS data and provide a basis for the preliminary characterisation of unknown porphyrins. More than one hundred individual porphyrin components in the C_{27}–C_{37} range have been characterised by MS and KRI in the Boscan crude oil and at least forty in the C_{28}–C_{35} range for Gilsonite on the basis of the single ion mass fragmentograms (*e.g.* Fig. 6) and the full mass spectra recorded for individual scans (*e.g.* Fig. 6). The mass fragmentograms are interpreted as corresponding to porphyrins of a given molecular formula. However, as few standard compounds are available for confirming the peak

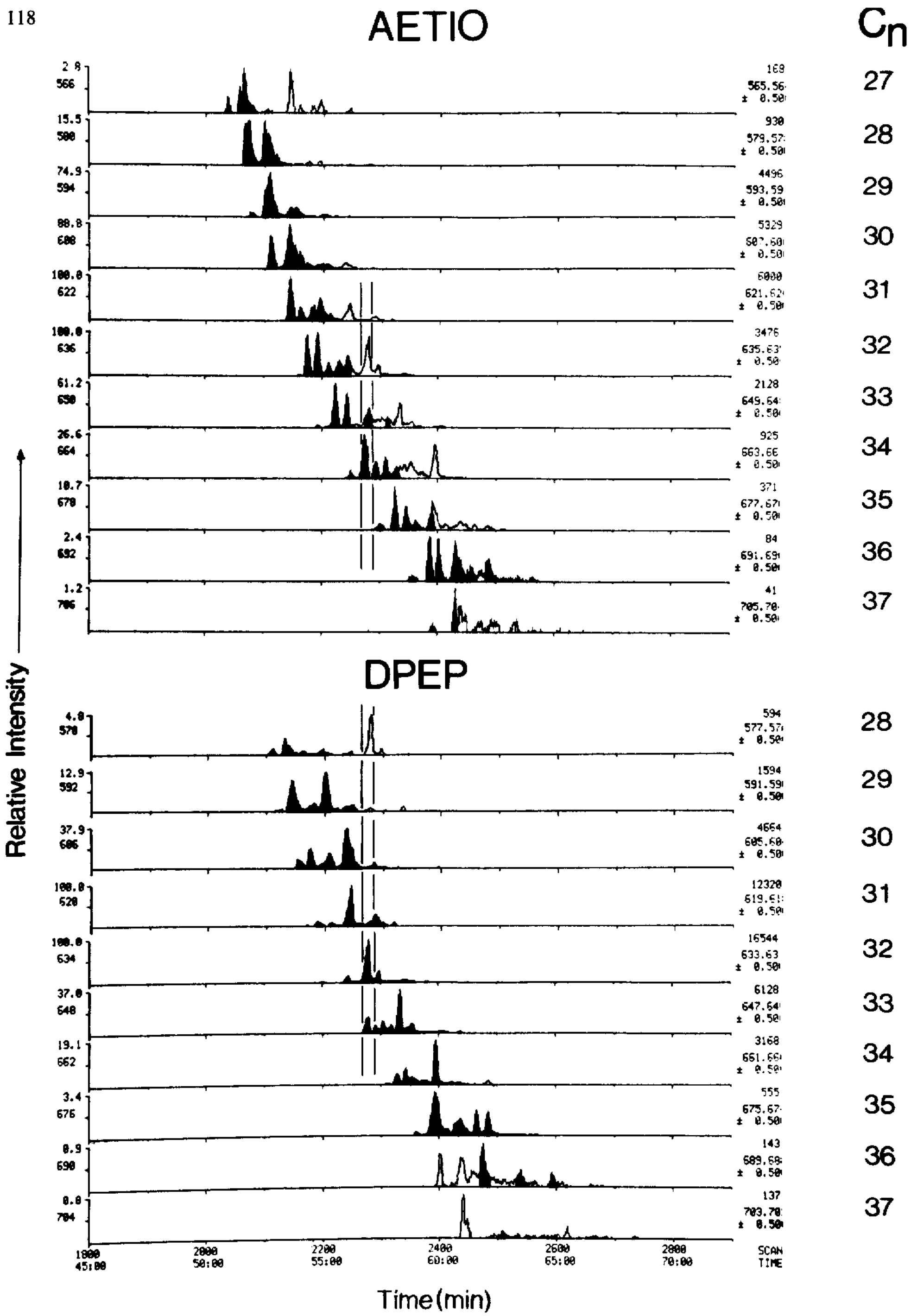

Fig. 4. Mass fragmentograms for the aetio and DPEP type porphyrins of the Boscan crude oil. The fragmentograms are selected on the basis of the calculated masses of the intense $(M-131)^+$ ions listed in Table I. All the peaks have been screened through their mass spectra using the procedure shown in Fig. 5. Those corresponding to genuine $(M-131)^+$ fragment peaks are shaded. The computerised GC–MS conditions are as for Fig. 3. Figs. 5 and 6 show the summed mass spectrum for the scans within the window indicated by the vertical lines.

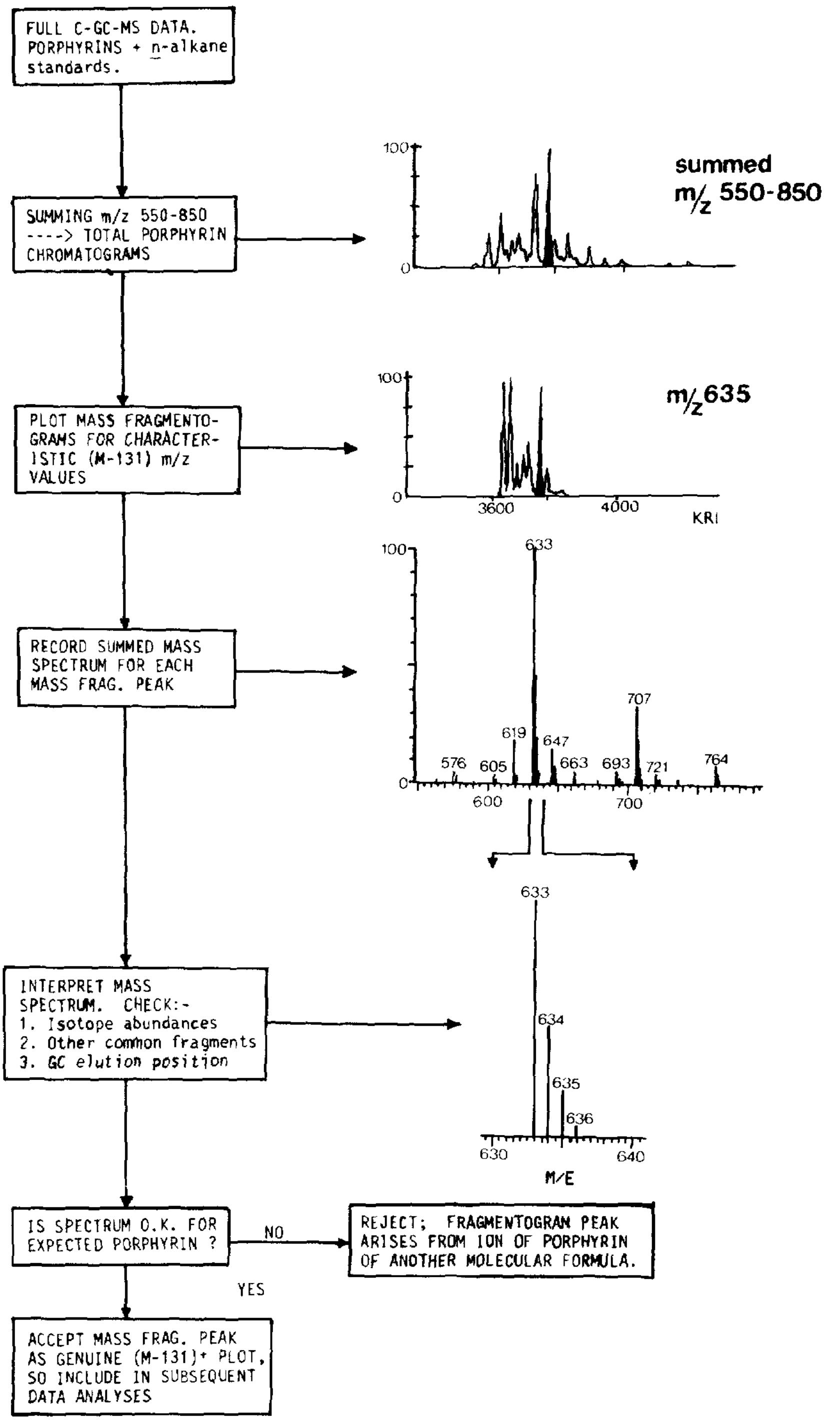

Fig. 5. Schematic representation of the interpretation procedure for data obtained by the computerised GC–MS of petroporphyrins as their $(TBDMSO)_2Si$ derivatives. This screening procedure is employed to check whether or not peaks occurring in the single ion mass fragmentograms are genuine $(M-131)^+$ fragments or arise in some other way. See text for full description of procedure.

TABLE II

A SUMMARY OF PROCESSES GIVING RISE TO POSSIBLE MISINTERPRETATION OF PEAKS IN THE GC–MS ANALYSIS OF PORPHYRIN $Si(OTBDMS)_2$ DERIVATIVES

No.§	*Actual ion*	*Process*	*Apparent ion**,***	*Example*				
				m/z	*Actual species**	*Elemental comp. of actual ion***	*Apparent species**	*Elemental comp. of apparent ion***
I	M−131+2	$^{13}C_2$isotope peak of M-(OTBDMS) ion	Same C_{No}, 1 series higher	635	$C_{32}D$	$^{13}C_2{}^{12}C_{36}H_{49}N_4OSi_2$	$C_{32}A$	$^{12}C_{38}H_{51}N_4OSi_2$
II	M−131−2	Loss of 2 × H? from M-(OTBDMS) ion	Same C_{No}, 1 series lower	631	$C_{32}D$	$^{12}C_{38}H_{47}N_4OSi_2$	C_{32}D-D	$^{12}C_{38}H_{47}N_4OSi_2$
III	M−188+1	^{13}C isotope peak of M-(OTBDMS)-*tert.*-butyl ion	Same series, 4 C_{Nos} lighter	577	$C_{32}D$	$^{13}C^{12}C_{33}H_{40}N_4OSi_2$	$C_{28}D$	$^{12}C_{34}H_{41}N_4OSi_2$
IV	M−57+2	$^{13}C_2$ isotope peak of M-*tert.*-butyl ion	3 Series higher, 5 C_{Nos} heavier	669	$C_{29}A$	$^{13}C_2{}^{12}C_{35}H_{51}N_4O_2Si_3$	C_{35}R-D	$^{12}C_{41}H_{49}N_4OSi_2$
V	M−57	Loss of *tert.*-butyl from $M^{+\cdot}$	2 Series higher, 5 C_{Nos} heavier	633	C_{27}R-A	$^{12}C_{35}H_{41}N_4O_2Si_3$	$C_{32}D$	$^{12}C_{38}H_{49}N_4OSi_2$
VI	M−131−15+1	^{13}C isotope peak of M-(OTBDMS)-Me ion	Same series, 1 C_{No} lighter	619	$C_{32}D$	$^{13}C^{12}C_{36}H_{46}N_4OSi_2$	$C_{31}D$	$^{12}C_{37}H_{47}N_4OSi_2$
VII	M−57−2	Loss of 2 × H? from M-*tert.*-butyl ion	1 Series higher, 5 C_{Nos} heavier	633	C_{27}D-D	$^{12}C_{35}H_{41}N_4O_2Si_3$	$C_{32}D$	$^{12}C_{38}H_{49}N_4OSi_2$
VIII	M−131+4	$^{13}C_4$ isotope peak of M-(OTBDMS) ion	Same C_{No}, 2 series higher	635	C_{32}D-D	$^{13}C_4{}^{12}C_{34}H_{47}N_4OSi_2$	$C_{32}A$	$^{12}C_{38}H_{51}N_4OSi_2$
IX	M−188+3	$^{13}C_3$isotope peak of M-(OTBDMS)-*tert.*-butyl ion	1 Series higher, 4 C_{Nos} lighter	579	$C_{32}D$	$^{13}C_3{}^{12}C_{31}H_{40}N_4OSi_2$	$C_{28}A$	$^{12}C_{34}H_{43}N_4OSi_2$
X	M−188−15	Loss of (OTBDMS), *tert.*-butyl and Me from $M^{+\cdot}$	1 Series lower, 5 C_{Nos} lighter	563	$C_{32}A$	$^{12}C_{33}H_{39}N_4OSi_2$	$C_{27}D$	$^{12}C_{33}H_{39}N_4OSi_2$

* C_{No} calculated for free-base porphyrin, *i.e.* ignoring TBDMS groups. Series in descending order of weight for given C_{No}:

Higher | A = Aetio-type porphyrin
| D = DPEP-type porphyrin
| D-D = Di-DPEP-type porphyrin
| R-A = Rhodo-aetio-type porphyrin
Lower | R-D = Rhodo-DPEP-type porphyrin.

** Calculated using only ^1H, ^{12}C, ^{13}C, ^{14}N, ^{16}O, ^{28}Si; all other isotopes <0.4% except ^{29}Si (4.71%), ^{30}Si (3.12%)

*** The apparent ion is the M−131 ion isobaric with the actual ion.

§ Only processes Nos. 1–III are significant enough to cause problems in data interpretation.

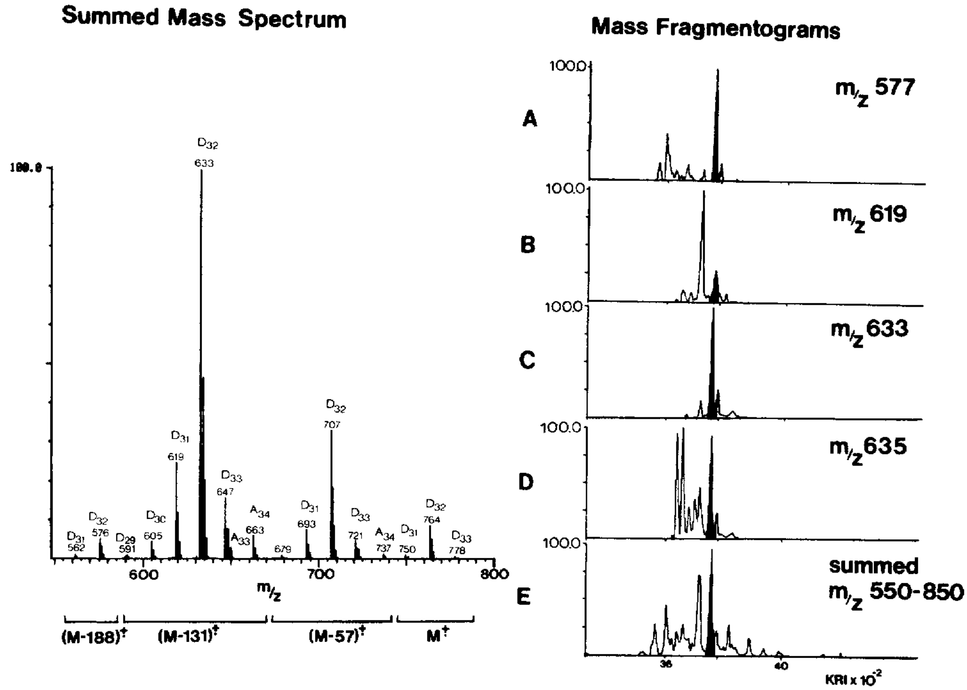

Fig. 6. Selected mass fragmentograms and fully interpreted summed mass spectrum for the shaded peak (KRI 3755–3800, the retention window indicated in Fig. 4) of the Boscan total porphyrin chromatogram (trace E). Misassignment of mass fragmentogram peaks may occur in the absence of careful examination of the mass spectra. The mass fragmentograms A and D contain peaks which do not correspond to the characteristic $(M-131)^+$ fragment ions but arise from ^{13}C isotope peaks of lower mass fragment ions. In fragmentogram A (*m/z* 577; Table I), the major peak (shaded) corresponds, not to the $(M-131)^+$ of a C_{28} aetio, but to the ^{13}C isotope peak of a known fragment ion $(M-188)^+$ of a C_{32} DPEP component. In fragmentograms B and C (*m/z* 619 and 633, respectively; Table I), the shaded peaks correspond to the $(M-131)^+$ ions of genuine C_{31} and C_{32} DPEP components, respectively. In D (*m/z* 635; Table I), the shaded peak arises, not from a C_{32} aetio, but is the $((M-131)+2)^+$ isotope peak of the $(M-131)^+$ of the C_{32} DPEP eluting at that point. E is the total porphyrin chromatogram for this Boscan run. The GC–MS conditions are as for Fig. 3.

identities by co-injection, other means of identification must be sought. One approach which is presently being explored, is to use the numerical listings of KRI to produce plots of KRI against C_n for the various structural types of porphyrin. Fig. 8 shows examples of such plots, produced with the aid of a computer graphics program, for the aetio and DPEP type porphyrins of Gilsonite and Boscan. These plots reveal that many of the points lie on near parallel straight lines, and hence presumably correspond to homologous or pseudo-homologous series of porphyrin derivatives. These straight-line relationships are commonly found with chromatographic data for homologous or pseudo-homologous series of compounds. If the linear relationships of Fig. 8 are valid, it implies that a retention difference equivalent to about 40 KRI units (*i.e.* 0.4 of one "carbon unit" in an *n*-alkane series) exists between subsequent members of the porphyrin series. A similar per-carbon increment was seen for the C_{29}, C_{32} and C_{36} standards previously reported[21], however, as to whether or not these standards represent members of a pseudo-homologous series analogous to those

```
____________________* RRI:   GC-MS MAP *____________________
 FILE:   PGF0533*633. RI
 FOR:
 NUMBER PKS:              11.              REF  AREA:
 LARGEST PK:          140466.              REF  QUAN:
 TOTAL AREA:          206308.              REF  UNIT:
 SUBJ:   RPE
 SCAN RANGE: 2000 TO   2800                ANYL:
 MASS RANGE:  550 TO    850                ACCT: 0533
 SECS. /SCAN:    1. 50                     INST: FINN
 TIME:                                     DATE: 03/26/83
 CNDS: 50-150/49, 150-290/3 ON COL INJ
 SAMP:   BOSCAN SI(OTBDMS)2'S +BP ALKANES
```

PEAK AREA	DATA SCAN	KRI	MOST ABUNDANT FRAGMENT MASSES 1ST	2ND	3RD	4TH	HIGH MASS	
3364.	2202	3675. 0	591	621	605	592	844	☆
1045.	2227	3708. 0	649	635	650	619	782	
19180.	2246	3733. 3	619	620	693	633	850	☆
140466.	2282	3781. 3	633	635	707	708	850	☆
25894.	2299	3803. 1	633	635	707	619	767	☆
907.	2311	3815. 6	647	649	633	664	779	
5351.	2341	3846. 9	633	647	661	634	793	☆ (bracketed with next row)
5628.	2345	3851. 0	661	633	663	647	794	
3235.	2359	3865. 6	647	649	662	633	779	
695.	2380	3887. 5	662	633	647	736	736	☆ (bracketed with next row)
532.	2383	3890. 6	633	661	663	647	738	

AREA FILTER=   0. 500998E 3

Fig. 7. Output from relative retention index listing (RRIL) program for the C_{32} DPEP porphyrins of Boscan crude oil. The KRI and peak area calculations are based on the M − 131 (*m/z* 633) ion current profiles (= mass fragmentograms on a KRI scale). After screening through the fully interpreted mass spectra (Figs. 5 and 6) these data can be used to generate Kovat's plots of KRI *vs* porphyrin C_n (Fig. 8) and relative abundance distribution profiles (Fig. 9). The components in the *m/z* 633 list corresponding to genuine C_{32} DPEP (M − 131) peaks are asterisked.

observed in the geological mixtures is as yet unknown. In spite of this uncertainty it is notable that relating the components in any manner other than that shown in Fig. 8 produces a considerable discrepancy between the observed per-carbon increment and the value of 40 KRI units predicted during previous investigations[21].

The plots of KRI *vs.* C_n reveal a much larger number of series for Boscan than Gilsonite, *e.g.* at least six series of aetio porphyrins may be present in Boscan compared to only three in the case of Gilsonite. The geochemical significance of these differing complexities is presently under study. This technique offers considerable potential for classifying the porphyrins beyond the level of gross structural type, which is based on molecular formula alone. The apparently linear relationships are under detailed study by co-injection with the available derivatised porphyrins of

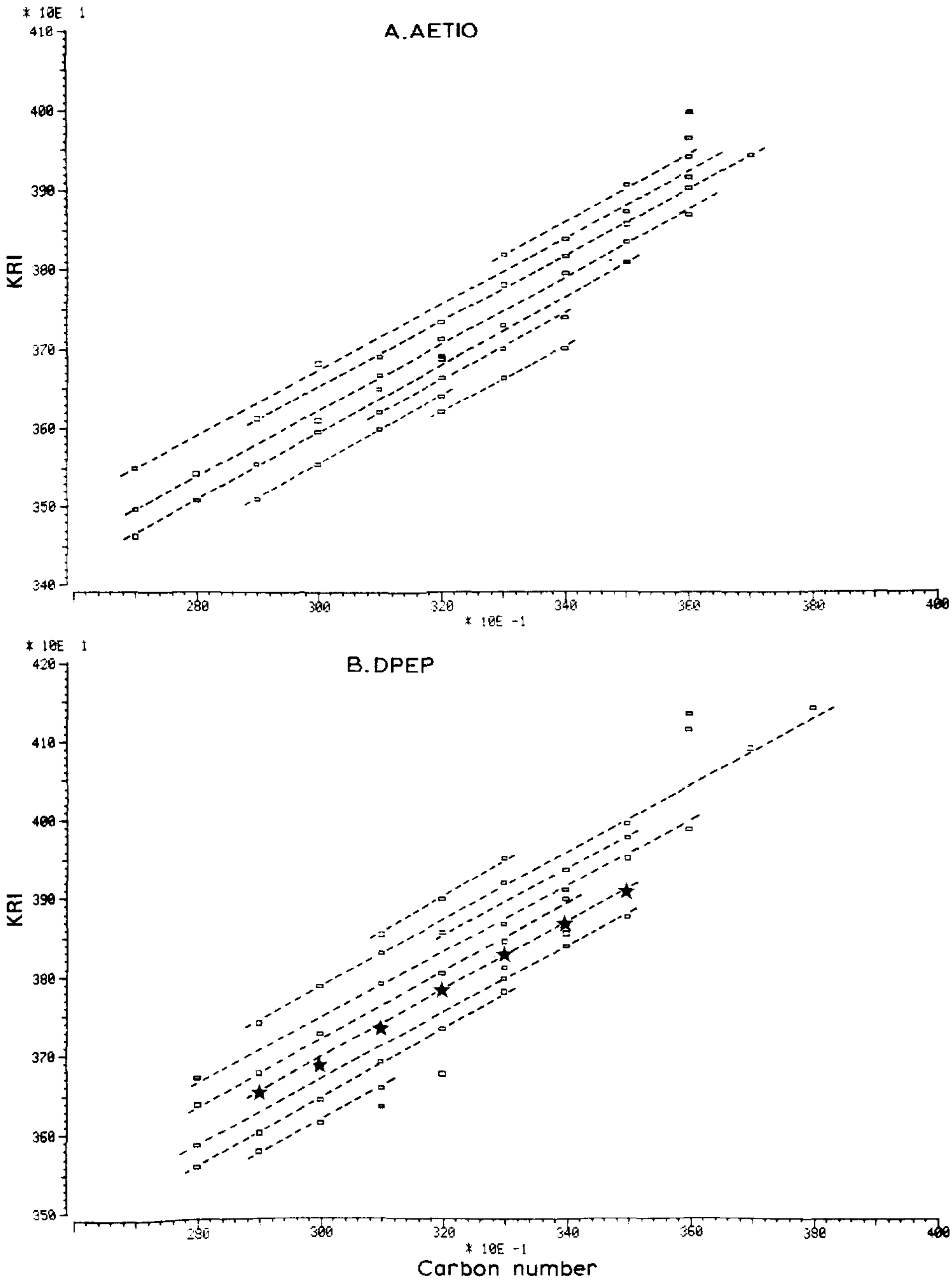

Fig. 8. Plots of C_n *vs.* KRI for (A) the aetio, and (B) the DPEP porphyrins of Boscan crude oil, as their $(TBDMSO)_2Si(IV)$ derivatives. Parallel or near-parallel lines can be drawn linking individual components in presumptive homologous or pseudo-homologous C_n series. Experimental details are the same as for Fig. 3. The relative intensity distribution profiles for the isomeric C_{32} DPEP porphyrins and the most abundant pseudohomologous series (asterisked) are shown in Fig. 9A and B, respectively.

known structure, as part of a major effort to characterise the various pseudo-homologous series of porphyrins which presumably generate these linear sequences. The few alkyl porphyrins of known structure presently available may be employed to explore the true nature of the homologous or pseudo-homologous series apparent in Fig. 8. Co-injection of derivatives of at least two structurally related porphyrins resulting in co-elution of these porphyrins with components of a suspected homologous series would provide excellent evidence for a structural relationship between all the components comprising that particular linear sequence.

Some indication of the diversity of isomeric structures possible for a given molecular formula has come from recent findings concerning the C_{32} DPEP type petroporphyrins; three structural isomers have already been characterised bearing 5, 6 and 7 membered isocyclic rings (structures 2, 7 and 8 respectively)[11–13]. In an independent investigation[28], three homologous DPEP structures related to structure

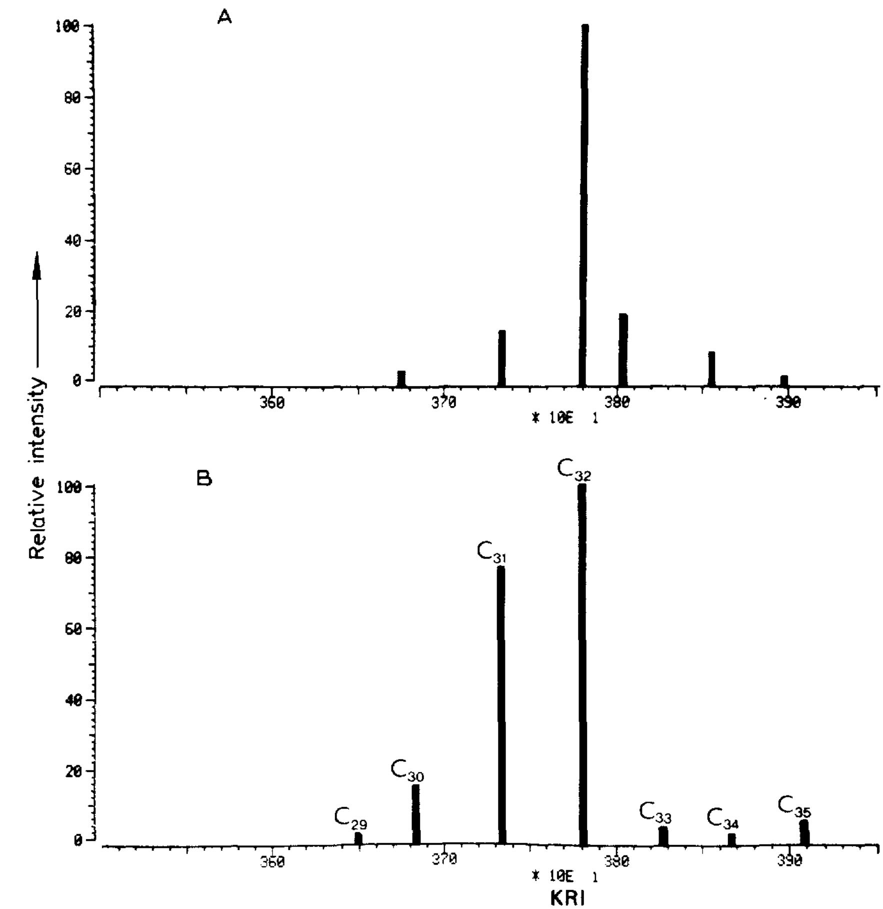

Fig. 9. Distribution profiles for isomers of single carbon number [C 32 DPEP isomers (A)], and a pseudo-homologous series [DPEP series (B)], of porphyrins of Boscan crude oil. The distribution profiles are for the C_{32} DPEP isomers and the pseudo-homologous series asterisked in Fig. 8. These profiles are derived from the MS ion intensity data (Fig. 7) and plotted on KRI scales of GC elution order. The vertical axes are a relative intensity scale, normalised to the major C_{32} DPEP as 100%.

8 have now been characterised. These and other investigations of structurally isomeric and pseudo-homologous petroporphyrins partially explain the large number of homologous or pseudo-homologous petroporphyrin series and their C_n ranges. Once these series have been more fully assigned, computerised GC–MS will offer a very powerful method for the qualitative analysis of petroporphyrin distributions.

Quantitative analysis

The ion intensities which are included in the listings of peak data (Fig. 7) allow quantitative assessment of the petroporphyrin composition. These ion intensities provide input for graphics programs which generate histograms which may take the form of distribution profiles for either isomers of a single carbon number (Fig. 9A) or a pseudohomologous series (Fig. 9B). The quantification at this stage is relative rather than absolute owing to the lack of pure standards. However, the relative ion currents of the various structural types of porphyrin derivative are not expected to differ appreciably. Such histograms offer a convenient and, where comparable GC conditions (stationary phase and programme conditions) are maintained, accurate means of comparing the petroporphyrins of related samples for the purposes of geochemical analysis. Examples of these histograms, based on the carefully processed mass fragmentograms, are shown in Fig. 9A and B for the porphyrins of Boscan. They emphasise the multiplicity of isomers for a given C_n and the wide variation in their relative abundances.

Both these latter distributions, and those for the pseudo-homologous series, provide a means of "fingerprinting" geological samples. Variations in the abundance of key components, as measured by the ion intensity data, offer sensitive indicators of geological and palaeo-environmental change and are presently the subject of detailed investigations in these laboratories.

Selectivity/non-selectivity of the analytical procedures

The petroporphyrin mixtures comprise a variety of structural types of alkyl porphyrin and the possibility of selectivity in the extraction, derivatisation and GC–MS procedures must be considered. Thorough investigations of the demetallation–extraction procedure have shown it to be efficient ($>85\%$) and non-selective with respect to the major structural types of alkyl petroporphyrin (*i.e.* aetio and DPEP). The efficiency of the derivatisation procedure has only been tested rigorously for synthetic aetio porphyrin standards (aetio-I and OEP), for which it is near quantitative ($>90\%$). The non-availability of other structural types has prevented further tests. This lack of standards has also prevented the GC recovery being tested rigorously for other than the aetio porphyrins. Using the Boscan crude oil, it has been possible to test the selectivity of the GC–MS technique by generating a single computer-summed mass spectrum over the full elution region of the GC–MS run for the porphyrin derivatives. In effect the pattern of the $(M - 131)^+$ ions in this spectrum has been compared with that of $M^{+\cdot}$ ions in the probe mass spectrum of the metalloporphyrins prior to demetallation, silicon insertion and derivatisation. The spectra confirm that the combined derivatisation and GC–MS procedure is non-selective, at least with respect to the major porphyrin structural types.

It has been reported[29] that Boscan porphyrins include compounds up to C_{60}. So far we have observed compounds up to C_{38}, if higher carbon numbers are present the very low abundance of higher homologues has precluded their detection by GC–MS in the present work.

Comparison of computerised GC–MS and HPLC of petroporphyrins

The normal-phase (SiO_2) HPLC separation of petroporphyrins as their free-bases is well developed. The attainment of good resolution relies on the different polarities (and basicities) of the porphyrin structural types and homologues. Careful trapping of peaks followed by probe MS and NMR experiments has shown that:

(1) The DPEP porphyrins are more polar (longer retention times (t_R)) than the corresponding aetio components.

(2) For a homologous series of a given porphyrin structural type, the t_R is inversely proportional to C_n (*i.e.* higher C_n homologues are less polar so elute earlier).

(3) For a given C_n the fully β-alkyl substituted porphyrins have a longer t_R than an isomer with a single free β-pyrrolic position.

(4) The structurally isomeric C_{32} aetio porphyrins (aetio porphyrins I–IV) when examined under either normal or non-aqueous reversed-phase conditions, reveal that only aetioporphyrin I can be partially resolved from the other three isomers.

In contrast to HPLC, the GC separation on apolar stationary phases reflects the differing volatilities of the various porphyrins. At least in part GC–MS analyses have shown that:

(1) The GC elution order of the various porphyrin structural types for a given C_n on OV-1 stationary phase is:

$$\underleftarrow{\text{aetio} < \text{DPEP} < \text{di-DPEP} < \text{rhodo-aetio} < \text{rhodo-DPEP}}_{\text{decreasing retention time}}$$

(2) For a homologous series of a given porphyrin structural type, the retention, as measured by retention index, is directly proportional to the C_n (*i.e.* the lower C_n homologues are the most volatile and elute earliest).

(3) GC is unable to resolve two of the fully alkyl substituted structural isomers of a C_{32} aetio porphyrin (aetio I and III) on the non-polar phase used here. However, as to whether any of the other structural isomers are separable is currently under investigation. The use of more efficient capillary columns may facilitate this type of separation. The different retention mechanisms effecting separation of the porphyrins, as their free-bases by HPLC and $(TBDMSO)_2Si(IV)$ derivatives by GC are clearly reflected in the reversal of molecular weight elution order of components of a homologous series when the two methods are compared.

As the HPLC analyses are performed on the free-base porphyrins an obvious advantage of this technique is the simpler sample preparation. Furthermore, the HPLC is presently capable of higher resolution than the GC technique. In spite of these notable advantages the LC–MS, in contrast to GC–MS, although demonstrated for free-base porphyrins, is not yet perfected.

The differing detection systems employed in the HPLC, GC and GC–MS analysis of petroporphyrins also warrant consideration. At present, HPLC relies exclusively on spectrophotometric detection, typically at the Soret band located at about 400 nm. While this is an intense absorption, its λ_{max} and extinction coefficient (ε) do vary according to alkyl porphyrin structural type[13,30,31], hence the profiles obtained by HPLC during the analysis of complex petroporphyrin mixtures are not accurate relative abundance distributions. In contrast, the GC profiles obtained using flame ionisation detection (FID), are truer relative abundance distributions. FID response factors have only been recorded for a limited number of alkyl porphyrin derivatives[21]. However, owing to the similarity in molecular composition and structure between the various types of porphyrin, their FID response factors should show little variation. Unfortunately though, while the GC profiles are accurate relative abundance plots for the petroporphyrins, the GC resolution is insufficient to provide useful information beyond a relatively crude fingerprint due to the extent of co-elution. However, computerised GC–MS is able to provide very detailed compositional information through the mass spectra and mass fragmentograms. As the ion yields of the porphyrin derivatives are dependent largely on the fragmentation of the derivatising group rather than the porphyrin nucleus itself, it follows that the ion yields of the $(M - 131)^+$ ions of various porphyrin structural types should be very similar. Indeed, the total porphyrin chromatograms obtained through computerised GC–MS, and through GC using FID are closely similar.

An obvious advantage of computerised GC–MS is its ability to resolve co-eluting components by MF and careful study of the full mass spectra. In contrast, confirmation of co-elution/non-co-elution in HPLC requires lengthy trapping and probe-MS analyses. Hence, computerised GC–MS currently offers a more powerful technique for petroporphyrin analysis. However, once fully developed and widely available, LC–MS should complement GC–MS as a routine technique for petroporphyrin analysis.

CONCLUSIONS

This paper has shown that alkyl petroporphyrins can be analysed by computerised GC–MS as their bis(trialkylsiloxy)silicon (IV) derivatives on apolar stationary phases. Owing to its more favourable GC–MS behaviour the TBDMS derivative is considered to be more amenable to routine analysis than the TMS. To date GC columns up to 25 m in length have been employed. The possibility of employing longer, more efficient GC columns and other, thermally stable GC stationary phases is being explored with the aim of improving GC resolution. Petroporphyrins are frequently highly complex mixtures; as a result the computerized GC–MS analysis yields a substantial volume of retention and MS data. Computerised data handling greatly simplifies the processing of these data. In addition to identifying the individual components (C_n and structural type) through their mass spectra, Kovat's type plots of KRI *vs.* C_n enable further classification of the porphyrins into a number of homologous or pseudo-homologous series for the aetio and DPEP porphyrins. The identities of the porphyrins comprising these proposed series are being checked by a programme of co-injections with porphyrin derivatives of known structure. The computer produced KRI and ion intensity data enables a quantitative presentation of the petroporphyrin data through histogram profiles for individual C_n or homologous series. This latter form of the data which is relative rather than absolute at this stage, will be of use in geochemical investigations.

The results of the analyses of the Gilsonite and Boscan petroporphyrins have revealed a complexity in their distributions inaccessible by other currently available techniques.

ACKNOWLEDGEMENTS

The authors thank Mrs. A. P. Gowar and Mr. C. L. Saunders for their invaluable assistance with the computerised GC–MS facilities. Morris Ashby Ltd. and the Shell Oil Co. are thanked for their gifts of Gilsonite bitumen and Boscan oil respectively, as is Dr. J. G. Erdman for his kind donation of the free-base aetio porphyrin compounds. The Science and Engineering Research Council are thanked for financial support (GR/B/04471) and a Research Studentship (J.P.G.), as are the British Petroleum Co. Ltd. (R.P.E. and C.S.H.) and the National Aeronautics and Space Administration (sub-contract from NGL-05-003-003, the University of California, Berkeley). The Natural Environment Research Council's grants (GR3/2951 and GR3/3758) provided GC–MS and MS computing facilities.

REFERENCES

1 S. E. Palmer and E. W. Baker, *Science*, 201 (1978) 49.
2 R. Bonnett and F. Czechowski, *Nature (London)*, 283 (1980) 465.
3 R. Bonnett and F. Czechowski, *Philos. Trans. R. Soc. London Ser. A.*, 300 (1981) 51.
4 J. W. Louda and E. W. Baker, *Initial Reports of the Deep Sea Drilling Project Vol. LXIII*, U.S. Govt. Printing Office, Washington, DC, 1981, p. 785.
5 E. W. Baker, *J. Amer. Chem. Soc.*, 88 (1966) 2311.
6 E. W. Baker, T. F. Yen, J. P. Dickie, R. E. Rhodes and L. F. Clarke, *J. Amer. Chem. Soc.*, 89 (1967) 3632.
7 A. J. G. Barwise and I. Roberts, in P. A. Schenck, J. W. de Leeuw and G. W. M. Lijmbach (Editors), *Advances in Organic Geochemistry 1983*, Pergamon Press, Oxford, submitted for publication
8 A. Treibs, *Justus Liebigs Ann. Chem.*, 509 (1934) 103.
9 A. Treibs, *Justus Liebigs Ann. Chem.*, 510 (1935) 42.
10 S. K. HajIbrahim, J. M. E. Quirke and G. Eglinton, *Chem. Geol.*, 32 (1981) 173.
11 J. M. E. Quirke, J. R. Maxwell, G. Eglinton and J. K. M. Sanders, *Tetrahedron Lett.*, 21 (1980) 2987.
12 G. A. Wolff, M. Murray, J. R. Maxwell, B. K. Hunter and J. K. M. Sanders, *J. Chem. Soc., Chem. Comm.*, (1983) 922.
13 G. A. Wolff, *Ph.D. Thesis*, University of Bristol, U.K., 1983.
14 W. H. McFadden, D. C. Bradford, G. Eglinton, S. K. HajIbrahim and N. Nicolaides, *J. Chromatogr. Sci.*, 17 (1979) 518.
15 P. J. Arpino and G. Guiochon, *Anal. Chem.*, 51 (1979) 612A.
16 D. B. Boylan and M. Calvin, *J. Amer. Chem. Soc.*, 89 (1967) 5472.
17 D. B. Boylan, Y. I. Alturki and G. Eglinton, in P. A. Schenck and I. Havenaar (Editors), *Advances in Organic Geochemistry 1968*, Pergamon Press, New York, 1969, p. 227.
18 P. J. Marriott, J. P. Gill, R. P. Evershed, G. Eglinton and J. R. Maxwell, *Chromatographia*, 16 (1982) 304.
19 R. Alexander, G. Eglinton, J. P. Gill and J. K. Volkman, *J. High Resolut. Chromatogr. Chromatogr. Commun.*, 3 (1980) 521.
20 P. J. Marriott, J. P. Gill and G. Eglinton, *J. Chromatogr.*, 236 (1982) 395.
21 P. J. Marriott, J. P. Gill and G. Eglinton, *J. Chromatogr.*, 249 (1982) 291.
22 G. Eglinton, R. P. Evershed and J. P. Gill, in P. A. Schenck, J. W. de Leeuw and G. W. M. Lijmbach (Editors), *Advances in Organic Geochemistry 1983*, Pergamon Press, Oxford, in press.
23 J. G. Erdman, *U.S. Patent*, 3,190,829 (1965).
24 E. J. Corey and A. Venkateswarlu, *J. Amer. Chem. Soc.*, 94 (1972) 6190.
25 H. van den Dool and P. D. Kratz, *J. Chromatogr.*, 11 (1963) 463.
26 M. A. Quilliam, K. K. Ogilvie and J. B. Westmore, *J. Chromatogr.*, 105 (1975) 297.
27 C. F. Poole, in K. Blau and G. King (Editors), *Handbook of Derivatives for Chromatography*, Heyden and Sons Ltd., London, 1978, p. 185.
28 C. J. R. Fookes, *J. Chem. Soc., Chem. Comm.*, (1983) 1474.
29 A. J. G. Barwise and E. V. Whitehead, in A. G. Douglas and J. R. Maxwell (Editors), *Advances in Organic Geochemistry 1979*, Pergamon Press, Oxford, 1980, p. 181.
30 K. M. Smith, *Porphyrins and Metalloporphyrins* , Elsevier/North-Holland Biomedical Press, Amsterdam, 1976, p. 876.
31 M. I. Chicarelli, personal communication.